Available online at www.derpharmachemica.com

ISSN 0975-413X
CODEN (USA): PCHHAX

Der Pharma Chemica, 2016, 8(12):184-197
(http://derpharmachemica.com/archive.html)

Synthesis, characterization, thermal and 3D molecular modeling studies of transition metal complexes supported by ONN / ONO tridentate Schiff base hydrazone

N. Kavitha and P. V. Anantha Lakshmi*

Department of Chemistry, University College for Women, Osmania University, Koti, Hyderabad, Telangana State, 500095, India

---

ABSTRACT

Studies on metal chelates with Schiff bases of dehydroacetic acid have received attention due to their excellent chelating capacity in modern coordination chemistry. The dehydroacetic acid is widely used as fungicide, herbicide and as preservative that has powerful antimicrobial affect against bacteria, yeast and particularly molds. This compound has several reactive functional groups and can serve as a reagent in organic synthesis. The complexes of Ni(II), Cu(II) and Zn(II) with Schiff base 3-(2-(1-(4-hydroxy-6-methyl-2-oxo-2H-pyran-3-yl) ethylidene) hydrazinyl)-2H-benzo[b][1,4]oxazin-2-one (HMOPE-HBO) derived from dehydroacetic acid (3-acetyl-4-hydroxy-6-methyl-2H-pyran-2-one) (AHMPO) and 3-Hydrazino-1,4-benzoxazine-2-one (HBO) have been synthesized. The ligand acts as tridentate ONN / ONO donor. The ligand was characterized by LC-MS, IR, ^{1}H NMR and electronic spectral studies. Characterization of the complexes has been done on the basis of elemental analysis, molar conductivity, magnetic studies, thermal studies, IR, electronic spectral techniques, ESR spectral studies etc. The 3D molecular modeling structures of the ligand and its metal complexes are obtained by using Argus lab software. The geometrical structures have been found to be square planar/ octahedral. Thermal studies show degradation pattern of the compounds.

Key words: tridentate ONN/ONO donor, square planar, ESR, magnetic studies, molecular modeling.

INTRODUCTION

Benzoxazines are an important class of N-containing heterocyclic compounds which exhibit a wide range of biological activity and are used as key structural motifs for the synthesis of various pharmaceutical agents as antifungal [1], antimicrobial [2], 5HT1A receptor agonists, anti-thrombotic and cardiovascular agents [3], normolipemic agents [4], inotropic chronotropic and coronary vasodilating agents, antirheumatic agents [5], serotonin-3(5HT3) receptor antagonists, neuropeptide y5 antagonists, neuroprotective agents, estrogen receptor β agonists, anti-mycobacterial agents and antidiabetic agents. Benzoxazines and their Schiff bases are found to be biologically active according to the survey but, metal complexes of benzoxazine derivatives have received less attention inspite of their potential metal binding properties and promising applicability's. Importance was hence given to study these systems in our laboratory.

One of the oxygen heterocyclic compounds (dehydroacetic acid) 3-acetyl-4-hydroxy-6-methyl-2H-pyran-2-one (AHMPO) was reported to be an excellent chelating agent and to possess excellent fungicidal, bactericidal, herbicidal and insecticidal activities [6, 7]. It is also a versatile starting material for the synthesis of a wide variety of heterocyclic ring systems [8, 9].

Interest in the study of Schiff base hydrazones has been growing because of their antimicrobial, anti-tuberculosis, and anti-tumor activity [10]. Schiff bases play an important role in inorganic chemistry, as they form stable complexes with many transition metal ions.

In view of the importance of such Hydrazones, we described here the synthesis of the Schiff base 3-(2-(1-(4-hydroxy-6-methyl-2-oxo-2H-pyran-3-yl)ethylidene) hydrazinyl)-2H-benzo[b][1,4] oxazin-2-one (HMOPE-HBO) derived from AHMPO and HBO and also synthesis and characterization of its Ni(II), Cu(II) and Zn(II) complexes. These metal complexes may have enhanced biological activity which may have importance in the applied medicinal chemistry.

MATERIALS AND METHODS

Organic solvents of analytical grade were purchased from Merck (India), other chemicals (ortho-dichloro benzene, oxalyl chloride, ortho-amino phenol, Hydrazine hydrate, dehydro acetic acid) used were purchased from Sigma Aldrich company and all metal chlorides were procured from SD Fine chemicals and were used without purification. ^{1}H NMR data was obtained on a varian 400 MHz Mercury plus spectrometer and Bruker Biospin Switzerland AVANCE-III 400 MHz FT digital NMR spectrometer using DMSO-d_6 at RT using Tetra methyl silane as internal standard. IR spectra were recorded using KBr discs in the region of 4000-400 cm^{-1} on Brucker optics Germany TENSOR 27 FTIR. Far IR spectrum was also recorded in the region of 750-250 cm^{-1} using IR Prestige-21 Shimadzu Spectrophotometer. Solid UV spectra were recorded on UV-3600 Shimadzu UV-Vis-NIR spectrometer with reflectance arrangement. CHN analysis was done using micro analytical techniques on a Thermo Finnigan Flash EA 1112 elemental analyzer. Shimadzu AA-6300 atomic absorption spectrophotometer was used to estimate metal contents. The electrical conductance was recorded using freshly prepared DMSO solutions (1×10^{-3} M) using Elico digital conductivity meter (model CM-180) having a dip type cell calibrated with KCl solution. Total chloride content was estimated by argentometry. A mass spectrum was recorded on a LCMS-2010A Shimadzu Japan spectrometer. The magnetic moments of the complexes were recorded on a Faraday magnetic susceptibility millibalance model: 7550, at RT using Hg [Co $(SCN)_4$] as the standard. The diamagnetic corrections were done using Pascal's constants and temperature independent paramagnetic corrections were computed [11]. The presence of coordinated water or crystal water was established by TGA studies using TGA Q 5000 V3.13 build 261 instrument. The mp was recorded for complexes by DSC studies using DSC Q 1000V9.9 build 303 instrument. ESR spectrum of Cu(II) complex was recorded on JEOL, JES-A200 ESR spectrometer at RT and liquid nitrogen temperature (LNT). The XRD was recorded in the range 5º - 80º 2θ values on a Rigaku Miniflex diffractometer. Using Argus lab software the possible geometry of the Schiff base and the complexes were evaluated.

Synthesis of Schiff base HMOPE-HBO

HMOPE-HBO was prepared by a three-step process involving the synthesis of 1, 4-Benzoxazine-2, 3-dione (BDO) [12] and 3-Hydrazino-1, 4-benzoxazine-2-one (HBO) [13].

To a solution of HBO dissolved in hot distilled water (25 mL) (0.01 M, 1.77 g), AHMPO (dehydroacetic acid) (0.01 M, 1.68 g) dissolved in minimum amount of hot distilled water was added slowly with stirring. The reaction mixture was then refluxed on a mantle for two hours. The ligand was collected as a pale yellow colored solid which was filtered while hot, washed repeatedly with distilled water, recrystallized using acetic acid and dried in vacuum.

Synthesis of metal complexes

The experimental procedure adopted for the synthesis of all the metal complexes is as follows:
To the methanolic solution (25 mL) of metal chloride [(0.005 M) 1.18 g Ni (II), 0.85 g Cu (II) and 0.68 g Zn (II)], DMSO solution of HMOPE-HBO (3.27 g, 0.01 M) (15 mL) was added with stirring. The pH of the solution was adjusted to 7-8 range using 10% methanolic ammonia solution. The reaction mixture was heated under reflux for 4 h on hot mantle. The bright colored metal complexes thus separated were filtered, washed successively with small amounts of distilled water, methanol and petroleum ether and dried in vacuum. The purity of the complexes was tested by TLC using different solvent mixtures.

RESULTS AND DISCUSSION

Characterization of HMOPE-HBO

The general view of the preparation of new Schiff base HMOPE-HBO is shown in Scheme 1. It was prepared by the condensation of one mole of 3-hydrazino-1, 4-benzoxazine-2-one with one mole of 3-acetyl-4-hydroxy-6-methyl-2H-Pyran-2-one (dehydroacetic acid).

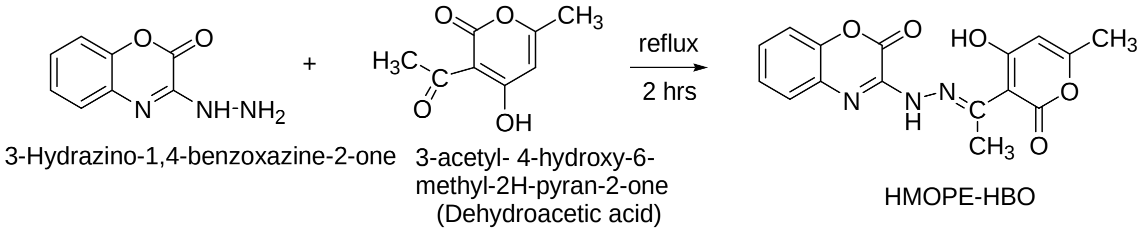

Scheme 1. Preparation of HMOPE-HBO

Yield: 80%, mp: > 300 ºC.
The elemental analysis (Found: C 58.87; H 4.08; N 12.75; Calcd: C 58.71; H 3.97; N 12.84 %) match the calculated values, indicating that the ligand has the molecular formula $C_{16}H_{13}N_3O_5$. The data also suggests 1:1 condensation of dehydroacetic acid with 3-hydrazino-1, 4-benzoxazine-2-one.

The LCMS of the ligand shows a peak at m/z 328 attributed to M+1 peak which corresponds to the molecular weight of the ligand 327.

^{1}H NMR spectrum of HMOPE-HBO was recorded in DMSO-d6. The chemical shifts (δ) are given in ppm downfield from tetra methyl silane represented in Figure 1. The spectrum shows characteristic signals due to -NH and enolic -OH. The spectrum shows signals between δ 6-8 ppm which can be due to aromatic protons of HMOPE-HBO [14]. The methyl protons of lactone ring (OC-CH_3 protons) resonate at δ 2.56 ppm as singlet [15, 16] & singlet appeared at δ 2.13 ppm is attributed to -CH_3 group on the azomethine carbon (-N=C-$\underline{C}H_3$) [17]. A short and broad singlet at δ 15.8 ppm can be attributed to proton of OH group [15]. The spectrum also shows a sharp singlet attributed to NH proton at δ 10 ppm. A signal at δ 6.4 ppm can be assigned to the proton of dehydroacetic acid moiety and the aromatic protons of benzoxazine are seen as a multiplet and a doublet at δ 7.1-7.42 and 7.8 ppm respectively [16]. The integration of each signal matches with the expected structure and the results have been substantiated by D_2O exchange studies.

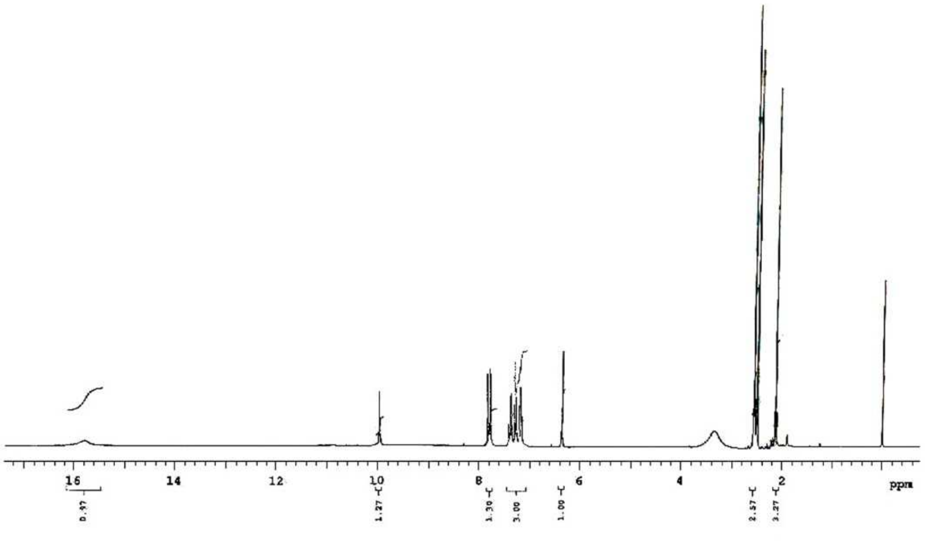

Figure 1. ^{1}H-NMR spectrum of HMOPE-HBO

The IR spectrum of HMOPE-HBO presents a broad peak at 3307 cm^{-1} corresponding to ν (OH) (enolic), a sharp peak at 3208 cm^{-1} can be assigned to ν (NH). The ν (C-O) (enolic) of ligand is observed at 1362 cm^{-1}. 2925 cm^{-1} band observed is due to aromatic CH stretching, the peak 2854 cm^{-1} may be ascribed to aliphatic CH symmetric stretching, a very sharp peak noticed at 1484 cm^{-1} can be for ν (C=C) stretching frequency of aromatic ring [18] and 1442 cm^{-1} peak may be due to ν (CH) asymmetric bending mode of methyl group [19]. The strong band noticed at 1685 cm^{-1} can be attributed to ν (C=O) of lactone carbonyl group [13, 20]. The spectrum also presents two short sharp bands at 1572 cm^{-1} [21] and 1554 cm^{-1} corresponding to ν (C=N) of both free and ring azomethine groups respectively. The signal at 999 cm^{-1} is the vibration of ν (N-N) moiety [22].

The electronic spectrum of HMOPE-HBO solid sample was recorded in the range of 200-1600 nm. It showed absorption bands at 49504 - 49019 cm^{-1}, 37037, 36630, 32362, 30959, 30487, 29154 and 28169 cm^{-1}. The bands in the region 49504 - 49019 cm^{-1} can be due to the π-π* transitions of substituted benzene moiety of the ligand. The bands at 37037, 36630 cm^{-1} can be attributed to the n-π* transitions of benzoxazine moiety and hydrazine side chain. The band at 32362 cm^{-1} is due to n-π* of enolic functional group. The band at 30959 and 30487 cm^{-1} is due to the transition of lactone carbonyl groups of dehydroacetic acid and benzoxazine moieties respectively. The band seen at 29154 cm^{-1} is assigned to π-π* transition of ring azomethine and 28169 cm^{-1} to n-π* of free azomethine group [23].

Molecular Modeling Studies of HMOPE–HBO

The ligand geometry was evaluated using molecular calculation with arguslab software (www.arguslab.com). The molecule is built and geometry optimization was done using quantum mechanics based AM1 (Austin Model 1) approximation and also molecular orbital calculations were performed. The Self consistent field (SCF) energy value and heat of formation ΔH_f for the optimized geometry are given below. The electron density surfaces of highest occupied molecular orbitals (HOMO) and lowest unoccupied molecular orbitals (LUMO) for the ground state of the ligand are obtained.

Final SCF Energy = -102555.3504 kcal/mol
Heat of Formation = -65.3238 kcal/mol

Characterization of metal complexes

All the complexes are colored, quite stable to air and moisture and are insoluble in most of the polar and nonpolar solvents, but are sparingly soluble in DMSO. All the complexes of HMOPE-HBO show decomposition without melting. Yield of complexes: Ni (II) - 62%, Cu (II) - 70%, Zn (II) - 73%.

Elemental analysis of metal complexes

The analytical data of all the complexes is presented in the Table 1.

The analysis of metal, carbon, hydrogen, nitrogen and chloride give the following formulae- $NiC_{32}H_{34}N_6O_{15}$, $CuC_{16}H_{16}N_3O_7Cl$ and $ZnC_{32}H_{31}N_6O_{13.5.}$ Elemental analysis shows 1:2 metal to ligand ratio in Ni (II) and Zn (II) complexes and 1:1 in Cu (II) complex. The presence of one chloride ion is also indicated in Cu (II) complex.

Table 1. Analytical data and physical properties of HMOPE-HBO complexes

Complex with Mol. Formula	Mol. Wt.	Color	d.pt. (°C)	Elements (found) % Calc.					Λ_m (Ω^{-1} cm^2 mol^{-1})
				M	C	H	N	Cl	
$[Ni(L)_2].5H_2O$ $NiC_{32}H_{34}N_6O_{15}$	800	Dark Brown	>300	7.33 (6.49)	48.1 (47.58)	4.24 (4.23)	10.5 (10.34)	_	5.7
$[Cu\ L\ Cl].2H_2O$ $CuC_{16}H_{16}N_3O_7Cl$	460	Dark Brown	>300	13.81 (13.79)	41.73 (40.4)	3.47 (3.41)	9.13 (8.92)	7.71 (7.69)	10.7
$[Zn\ (L)_2].3.5H_2O$ $ZnC_{32}H_{31}N_6O_{13.5}$	780	Light Brown	>300	8.43 (8.17)	49.23 (49)	4.1 (4.08)	10.76 (10.66)	_	12

Molar Conductance

The conductivity measurements were recorded in freshly prepared 1×10^{-3} M dimethyl sulphoxide (DMSO) solutions and the molar conductivity values are given in Table 1. The data show negligible molar conductance values (5 to 12 mho cm^2 mole^{-1}) indicating that all the complexes are non-electrolytes [24, 25, 26, 27] which indicates the presence of one chloride ion within the coordination sphere of Cu (II) complex.

Thermal Analysis

Thermal behavior and decomposition pattern of the metal complexes was established by recording TGA /DTG and DSC curves. These are tabulated in Table 2. A representative thermogram of Ni (II) complex is given in Figures 2-3. The heating rates were suitably controlled at 10 °C min^{-1} under nitrogen atmosphere and the weight loss was measured from ambient temperature to 350 °C.

TGA analysis of Ni (II) complex elucidates the weight loss corresponding to the thermal transitions. The TGA scan showed weight loss of 11.61% (cal.11.25%) in the temperature range of 37.5-87.5 °C in single step most likely due to the loss of loosely bound 5 lattice water molecules. The DTG curve in the corresponding TGA imply loss of lattice water which is observed at 62.5 °C accompanied by further decomposition of the complex at higher temperatures [28, 29].

DSC of the Ni (II) complex shows decomposition of lattice water at 85.41 °C under an air flux represented by a large and broad peak. It is also indicating a very broad peak at 212.04 °C which may be due to the phase transition of the complex and above which it may undergo further decomposition without melting.

TGA analysis of Cu (II) complex was studied which shows a weight loss of 8.26% (cal.7.82%) in the temperature range of 37.5-80 °C in single step due to the loss of 2 lattice water molecules and a DTG curve in the corresponding TGA is observed at 58 °C for dehydration of water which leads to further decomposition of the complex.

DSC of the Cu (II) complex indicates the presence of crystalline water molecules in the complex where it exhibits decompostion of water molecules shown by a large and broad endothermic peak at 87.69 °C under an air flux [29]. The thermogram is also exhibiting a very broad peak at 231.89 °C which may be attributed to either some transition or reduction after which the decomposition of the complex without undergoing any melting process may be noticed.

TGA study of Zn (II) complex shows loss of crystalline water with a weight loss of 8.19% (cal.8.07%) in the range of 37-80 °C in a single step process attributed to 3.5 water molecules [29, 30]. The DTG peak of the complex further indicate loss of water noticed at 56 °C and decomposition of the complex at higher temperatures.

DSC of the Zn (II) complex is exhibiting a very large and broad endothermic peak at 82.75 °C contributing to the presence of crystalline water and indicating its decomposition. A broad endothermic peak seen at 206.48 °C may be associated with some phase transition or reduction. Further no peaks are noticed in the thermogram which shows that the complex decomposes without melting. The percentage weight loss in all the complexes is in agreement with the calculated values.

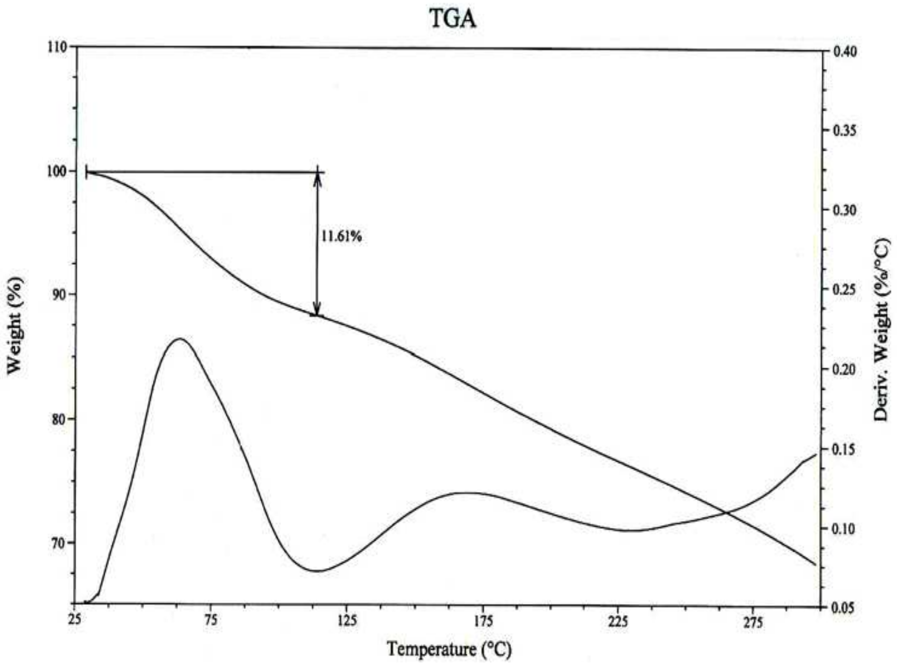

Figure 2. TGA of Ni (II) complex

Table 2. Thermo analytical results of HMOPE-HBO metal complexes

Complexes	TGA (°C)	DTG (°C)	Weight loss (%)		Assignment	DSC (°C) Endothermic peaks
			Calc.	Found		
Ni(II) complex	37.5 – 87.5	62.5	11.25	11.61	Single step with loss of 5 lattice water molecules.	85.41,212 °C
Cu(II) complex	37.5 – 80	58	7.82	8.26	Single step with loss of 2 lattice water molecules.	87.69, 232 °C
Zn(II) complex	37 – 80	56	8.07	8.19	Single step with loss of 3.5 lattice water molecules.	82.75, 206 °C

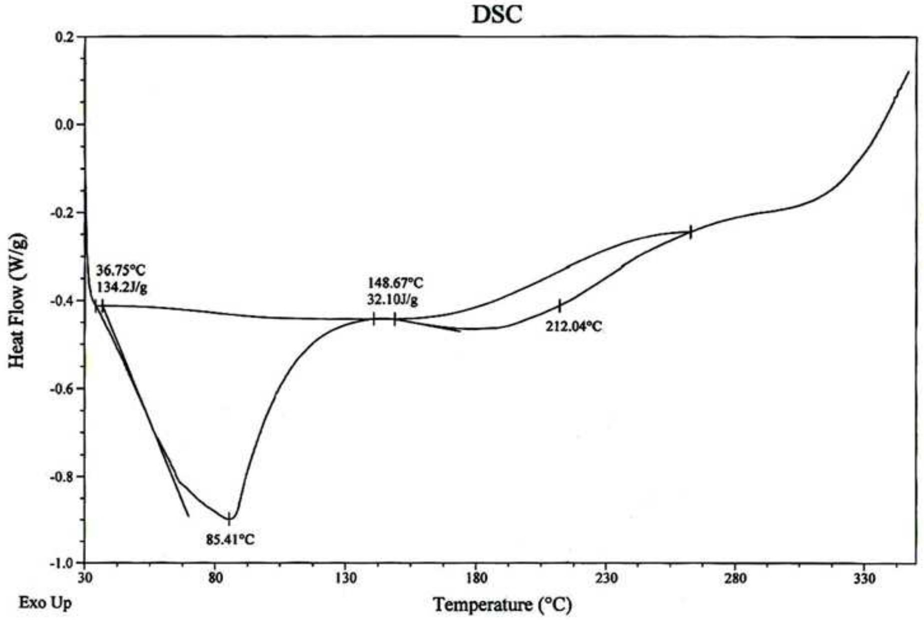

Figure 3. DSC of Ni (II) complex

Infrared Spectra

The significant bands in IR spectra of the ligand and the metal complexes are shown in Table 3.

The stretching frequencies of ν (OH), ν (NH), ν (C=O), ν (C=N) (free) and (ring), ν (C-O) and ν (N-N) in free ligand appear at 3307, 3208, 1685, 1572, 1554, 1362 and 999 cm^{-1} respectively.

The IR spectrum of all the complexes exhibit broad trough in the region of 3100-3500 cm^{-1} which are not seen in the ligand. This band can be assigned to a combination of ν (NH) and ν (OH) (of coordinated or lattice water) [16, 18, 31]. The changes in stretching frequencies due to ν (NH) and ν (OH) cannot be identified in the complexes as that region is merged with ν (OH) of water and appear as a broad band. As the complexes are isolated in neutral/weakly basic media the deprotonation of enolic group is definite which is further justified by the disappearance of old bands and formation of new broad bands in the complexes clearly indicating the deprotonation of OH group and coordination through enolic oxygen [19]. A band at 1362 cm^{-1} in this ligand assignable to ν (C-O) also has undergone a positive shift to 1403-1445 cm^{-1} in its complexes indicating coordination with the deprotonated hydroxyl oxygen which may be attributed to the drift of electron density from oxygen to the metal ions resulting in greater ionic character of the ν (C-O) bond and a consequent increase in ν (C-O) vibrational frequency [19]. The presence of lattice water in all the complexes is also proved by thermal analysis.

A strong band noticed at 1685 cm^{-1} attributed to lactone carbonyl group is found to be unchanged in Cu (II) and Zn (II) complexes ruling out the possibility of carbonyl oxygen participation in bonding with the metal ion [32]. Ni (II) complex showed a down ward shift of ν (C=O) to 1611 cm^{-1} indicating the involvement of carbonyl oxygen in metal bonding [20]. The down ward shift of the bands at 1572 cm^{-1} to a range of (10-14 cm^{-1}) and 1554 cm^{-1} to a range of (14-29 cm^{-1}) corresponding to ν (C=N) of Cu (II) and Zn (II) complexes respectively indicated the coordination of both free and ring azomethine nitrogen groups with metal ion [33, 34], which is further confirmed by the upward shift of ν (N-N) band of free ligand by 5-13 cm^{-1} in these complexes [35, 36]. Further the Ni (II) complex showed no change in the frequency corresponding to ν (C=N) (ring) confirming the participation of only free ν (C=N) in coordination by moving to negative shift.

The spectra of the complexes revealed the presence of medium intensity bands in the Far IR region- Ni (II) -532, 360 cm^{-1}, Cu (II) -576, 480 cm^{-1} and Zn (II) - 510, 493 cm^{-1} due to ν (M-N) and ν (M-O) vibrations respectively [37] and a peak at 349 cm^{-1} in Cu (II) complex is for ν (M-Cl) supporting its involvement in chelation. From the IR data, it has been concluded that the ligand HMOPE-HBO behaves as a monobasic tridentate ONN donor in Cu (II) and Zn (II) complexes coordinating through the deprotonated enolic oxygen and both nitrogens of ring and free azomethine groups, behaving differently with Ni (II) complex as tridentate ONO donor by coordinating with carbonyl oxygen, ν (C=N) (free) and enolic oxygen.

Table 3. Characteristic infrared frequencies of HMOPE-HBO complexes (cm^{-1})

Compound	ν (OH) / H_2O	ν(NH)	ν(C=O)	ν(C=N) (free)	ν(C=N) (ring)	ν(C-O) (enolic)	ν (N-N)	New Bands
HMOPE-HBO	3307	3208	1685	1572	1554	1362	999	_
Ni(II)	3500-3100(b)		1611	1562	1554	1403	1007	1302, 1170, 983, 949, 670, 532, 360.
Cu(II) Complex	3500-3185(b)		1681	1558	1525	1445	1012	1353, 1168, 1043, 951, 848,716, 661, 671, 576, 525, 480, 349.
Zn(II) Complex	3500-3100(b)		1681	1562	1468	1426	1004	1319, 1168, 947, 730, 713, 671, 534, 510, 493, 459, 408, 355.

Magnetic Moments

The magnetic susceptibility observed at room temperature, magnetic moments calculated and electronic spectral data are presented in the Table 4.

The Ni (II) complex exhibits effective magnetic moment value of 2.98 B.M. (2.5-3.5 B.M.) indicating a spin free octahedral configuration [17, 38]. The Cu (II) complex shows spin only magnetic moment of 1.88 B.M. which is in good agreement with the presence of one unpaired electron which is in close match with the required range (1.74-1.84 B.M.) [39, 40, 41] for d^9 systems and confirms mononuclear nature of the complex suggesting a square planar geometry. These geometries are further confirmed by electronic transitions. The Zn (II) complex is observed to be diamagnetic in nature [42].

Electronic Spectra

The electronic spectral data is used for assigning the stereochemistry of metal ions in the complexes based on the d-d transitions observed. The spectra of the complexes showed significant modifications giving evidence for the participation of the corresponding functional groups in coordination with the metal ions.

The UV-Vis peaks corresponding to π-π* and n-π* transitions in the ligand were observed to be shifted to either longer or shorter wavelength as a consequence of coordination with the metal ions confirming formation of HMOPE-HBO metal complexes.

π-π* and n-π* transitions of benzene, benzoxazine, enolic, lactone carbonyl group of benzoxazine and free azomethine groups of the ligand was seen to be shifted to longer wavelength of Ni (II) complex noticed at 49019-45045, 36764, 32051, 30211, 27777 cm^{-1} and that of lactone carbonyl of HMOPE group and ring azomethine group of the ligand seem to have not changed confirming their non-involvement in metal coordination. Both the transitions of lactone group of dehydroacetic acid moiety and benzoxazine in Cu (II) complex showed no change in absorption indicating its absence in metal interaction, a shift towards higher wavelength in π-π* and n-π* transitions of benzene and enolic group (48309-46948, 32051 cm^{-1}) and lower wavelength in n-π* transitions of benzoxazine moiety, ring and free azomethine groups (37735, 29940 and 29498 cm^{-1} resp.) clearly suggests there participation in metal interactions. Selective electronic spectral bands are given in Table 4.

Ni (II) complexes generally exhibit three absorption bands in the region 7000-13000, 13000-19000, and 20000-27000 cm^{-1} for (ν_1), (ν_2) and (ν_3) transitions [$^3A_{2g}$ (F) $\rightarrow$ $^3T_{2g}$ (F) (ν_1), $^3A_{2g}$ (F) $\rightarrow$ $^3T_{1g}$ (F) (ν_2), $^3A_{2g}$ (F) $\rightarrow$ $^3T_{1g}$ (P) (ν_3) respectively] [41, 43]. The electronic spectrum of the Ni (II) complex reveals four distinct bands at 26525, 7830, 13297, 25641 cm^{-1}. The band at 26525 cm^{-1} is assignable to charge transfer band and last three transitions are assigned to three spin allowed transitions $^3A_{2g}$ (F) $\rightarrow$ $^3T_{2g}$ (F) (ν_1), $^3A_{2g}$ (F) $\rightarrow$ $^3T_{1g}$ (F) (ν_2), $^3A_{2g}$ (F) $\rightarrow$ $^3T_{1g}$ (P) (ν_3) respectively. This suggests octahedral geometry around Ni (II) complex. The ratio ν_2/ν_1 is 1.69 which is required for a six coordinate octahedral Ni (II) system.

Cu (II) electronic spectrum presents three principle regions of absorption at 12048, 15673, 23923 cm^{-1} which can be attributed to $^2B_{1g}$ $\rightarrow$ $^2B_{2g}$ (ν_1), $^2B_{1g}$ $\rightarrow$ ^2E_g (ν_2) and $^2B_{1g}$ $\rightarrow$ $^2A_{1g}$ (ν_3) transitions respectively [19, 44], representing square planar structure [43]. A weak absorption at 24330 cm^{-1} may be due to charge transfer. The absence of any bands below 10000 cm^{-1} eliminates the possibility of tetrahedral geometry around the Cu (II) ion thus confirming a square planar geometry [45].

Zn (II) complex was assigned an octahedral geometry on the basis of analytical, conductance and other spectral data obtained, since no transitions are observed for it [42].

The ligand field parameters 10Dq and B have been calculated for Ni (II) complex. The Racah inter electron repulsion parameter B observed for the complex is less than that for the free ion. The nephelauxetic parameter β=B/B' is less than one [46]. All these observations suggest that the metal-ligand bond in the present complex is covalent in nature. The Racah inter-electron repulsion parameter (B) and nephelauxetic parameter β for Ni (II) complex (B = 488.12 cm^{-1} and β = 0.473) exhibits considerable amount of covalent character of the M-L bond and an octahedral geometry [41, 47].

Table 4. Magnetic and electronic spectral data of HMOPE-HBO complexes

Complex	μeff (B.M) (298K) Observed	μeff (B.M) Expected	UV-Vis Bands *ν* (cm^{-1})	Assignment	(ν_2) / (ν_1)	B (cm^{-1})	10Dq (cm^{-1})	β
Ni(II) complex	2.98	2.5-3.5	7830 13297 25641 26525	$^3A_{2g}(F) \rightarrow {}^3T_{2g}(F)$ $^3A_{2g}(F) \rightarrow {}^3T_{1g}(F)$ $^3A_{2g}(F) \rightarrow {}^3T_{1g}(P)$ Charge transfer	1.69	488.12	5467	0.47
Cu(II) complex	1.88	1.74-1.84	12048 15673 23924 24330	$^2B_{1g} \rightarrow {}^2B_{2g}$ $^2B_{1g} \rightarrow {}^2E_g$ $^2B_{1g} \rightarrow {}^2A_{1g}$ Charge transfer	–	–	–	–
Zn(II) complex	dia	–	–	–	–	–	–	–

ESR Spectra

The spectrum of Cu (II) complex of HMOPE-HBO in DMSO solution is measured at X-band frequency at 300 and 77 K which is given in Figures 4-5 respectively. The 300K spectrum shows an isotropic pattern, which is expected for Cu (II) in solution form, but the spectrum for the frozen solution shows usual anisotropic pattern which is expected for a powder sample.

The g tensor values of copper complex are used to derive its ground state. In square planar complexes, the unpaired electron lies in the $d_{x}2\text{-}_{y}2$ orbitals giving $^2B_{1g}$ as the ground state which is noticed for the Cu(II) complex $g_{\parallel} > g_{\perp} > g_e$ (2.0023) [48, 49, 50]. From the observed values it is clear that $A_{\parallel} = 95.70 > A_{\perp} = 44.68$; $g_{\parallel} = 2.16 > g_{\perp} = 2.04 > g_e$ (2.0023) and the ESR parameters of the complex coincides well with the related systems which suggests that the complex has square planar geometry and the system is axially symmetric. The fact that the unpaired electron lies predominantly in the $d_{x}2\text{-}_{y}2$ orbitals is also supported by the value of the exchange interaction term G estimated from the expression [51],

$$G = (g_{\parallel} - 2.0023) / (g_{\perp} - 2.0023)$$

If G > 4.0, the local axes are aligned parallel or only slightly misaligned. If G < 4.0, significant exchange coupling is present and the misalignment is appreciable. The observed value for the exchange interaction parameter for the Cu (II) complex (G = 3.72) which indicates considerable exchange interaction in the solid complex [52, 53, 54].

The molecular orbital coefficient (α^2) covalent in-plane σ - bonding is calculated using the equation [22].

$$\alpha^2_{Cu} = (A_{\parallel} / 0.036) + (g_{\parallel} - 2.0023) + 3/7\,(g_{\perp} - 2.0023) + 0.04$$

From the Table 5, it is clear that the in-plane σ - bonding parameter (0.49) α^2 is less than unity, which indicates that the complex has complete covalent character around the ligand. The observed $g_{\parallel}$ (2.16) value for the Cu (II) complex is less than 2.3, suggesting M-L bond a covalent character, which is in agreement with Kivelson and Neiman observations [22].

The spin orbit coupling constant, λ (79.31) cm^{-1}, is calculated by [22],

$$g_{av} = 1/3\,(g_{\parallel} + 2\,g_{\perp}) \text{ and } g_{av} = 2\,(1\text{-}2\,\lambda/10Dq).$$

It is less than that for the free Cu (II) ion (828 cm^{-1}). This reduction in λ from the free ion value is an evidence of M-L bond covalence [55, 36].The lower value of λ is indicating a considerable mixing of ground and excited state terms.

Table 5. Spin Hamiltonian parameters of Cu (II) complex of HMOPE-HBO in DMSO at 300 and 77K.

Complex	$g_{\parallel}$	$g_{\perp}$	g_{av}	G	$A_{\parallel} \times 10^{-4} (cm^{-1})$	$A_{\perp} \times 10^{-4} (cm^{-1})$	$A_{av} \times 10^{-4} (cm^{-1})$	α^2
[CuLCl].2H_2O	2.16	2.04	2.08	3.72	95.7	44.68	61.68	0.49

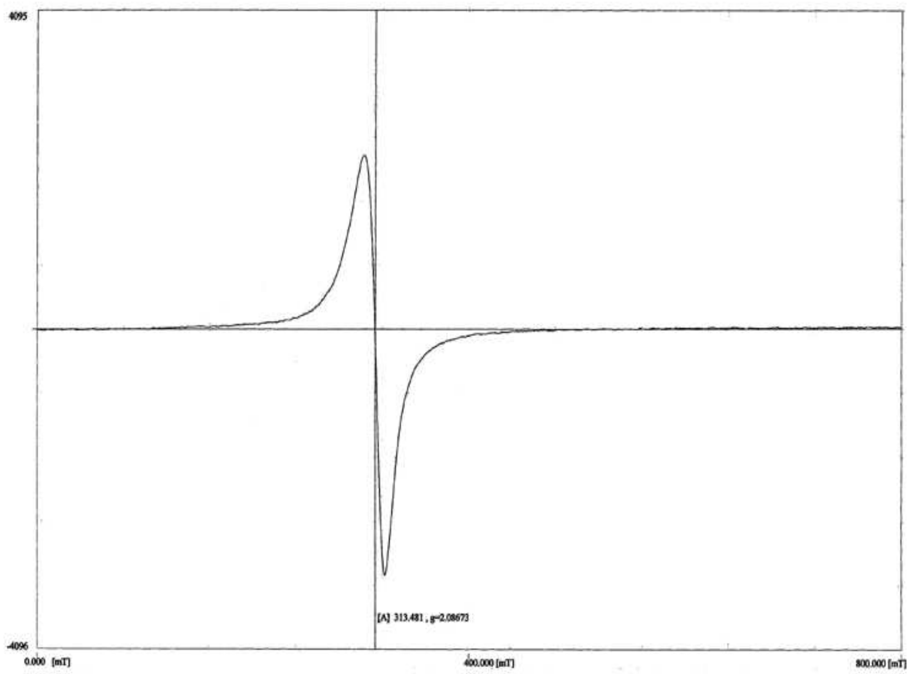

Figure 4. ESR spectrum of Cu (II) complex at R.T

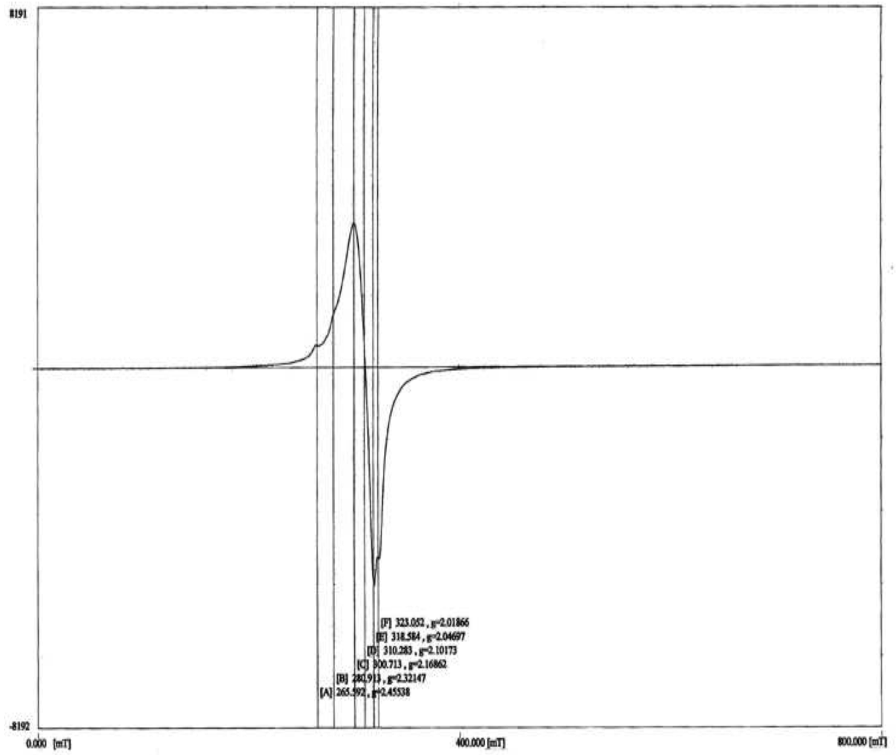

Figure 5. ESR spectrum of Cu (II) complex at LNT

Molecular Modeling Studies of HMOPE-HBO Metal Complexes

Various attempts were done for crystallization of the complexes with different solvents and mixtures and low temperature crystallization was also done which were unsuccessful in preparing a single crystal for crystallographic studies. In the absence of XRD crystal structure data the 3D structure of the molecules is important in analyzing the structure. The configuration possible for the Ni (II), Cu (II) and Zn (II) complexes were obtained using molecular mechanics (UFF) calculations as shown in Figures 6-8, the final geometry energy and the selected bond lengths for all the complexes are given below:

(a) Bond lengths of HMOPE-HBO Ni (II) complex (Å):
35 - 49 (N)-(Ni) 1.87

43 - 49	(O)-(Ni)	1.85
24 - 49	(O)-(Ni)	1.85
25 - 49	(O)-(Ni)	1.85
11 - 49	(O)-(Ni)	1.85
13 - 49	(N)-(Ni)	1.87

Geometry optimization:
Final geometry energy = 105.6788 kcal/mol

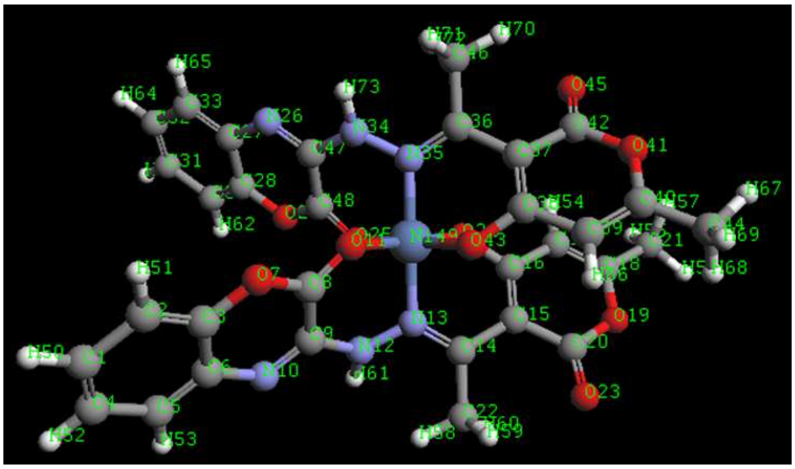

Figure 6. Molecular modeling structure of Ni (II) complex

(b) Bond lengths of HMOPE-HBO Cu (II) complex (Å):

24 - 37	(N)-(Cu)	2.02
11 - 37	(N)-(Cu)	2.02
9 - 37	(O)-(Cu)	2.02
37 - 38	(Cu)-(Cl)	2.41

Geometry optimization:
Final geometry energy = 108.0261 kcal/mol

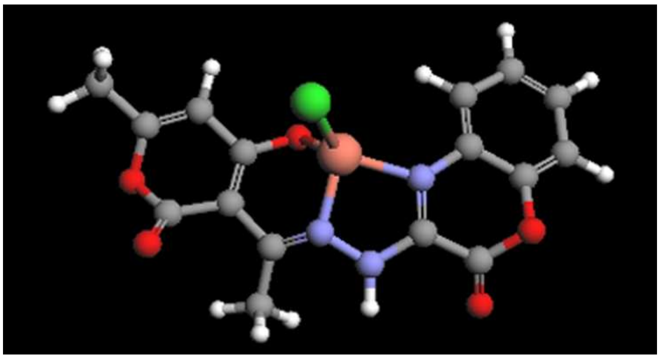

Figure 7. Molecular modeling structure of Cu (II) complex

(c) Bond lengths of HMOPE-HBO Zn (II) complex (Å):

25 - 73	(N)-(Zn)	1.89
37 - 73	(N)-(Zn)	1.89
46 - 73	(O)-(Zn)	1.86
22 - 73	(N)-(Zn)	1.89
11 - 73	(N)-(Zn)	1.89
7 - 73	(O)-(Zn)	1.86

Geometry optimization:
Final geometry energy = 401.2864 kcal/mol

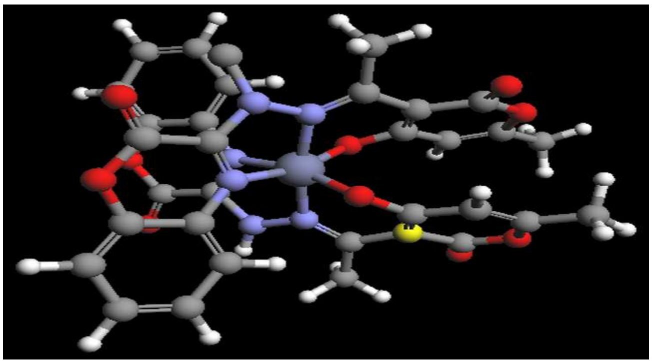

Figure 8. Molecular modeling structure of Zn (II) complex

Powder X-Ray Diffraction Studies

Single crystals of the Schiff base and the complexes under investigation could not be grown to get the XRD crystal structure and hence the powder diffraction data were obtained for structural characterization [28]. The X-ray diffractograms were recorded in the range 5º - 80º 2θ values, which are mentioned in the Figure 9. The pattern of XRD indicates that the ligand is crystalline in nature whereas its complexes are amorphous. The different pattern of the complexes compared with the ligand confirms the coordination of metal ion forming its metal complexes [56].

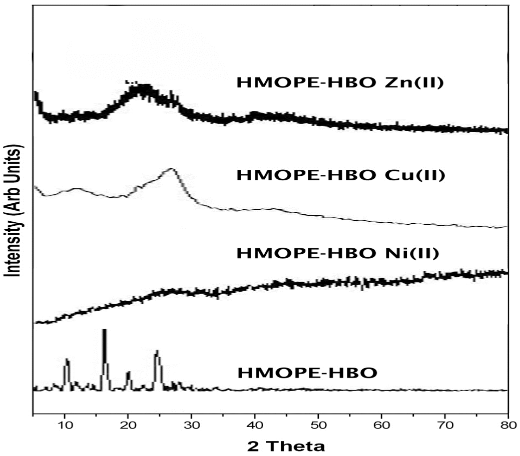

Figure 9. Powder XRD spectra of HMOPE-HBO complexes

CONCLUSION

Thus, in this study a new Schiff base HMOPE-HBO and its Ni (II), Cu (II) and Zn (II) complexes were synthesized and characterized. Based on the analytical data, electrical conductance, thermal studies, spectral studies and magnetic moments data octahedral geometries have been proposed for Ni (II) and Zn (II) complexes, wherein the ligand employs ONO and ONN donor sequences respectively. The Cu (II) complex shows a square planar geometry by binding to ONN donor atoms. The proposed structures of HMOPE-HBO metal complexes are presented in Figures 10-12.

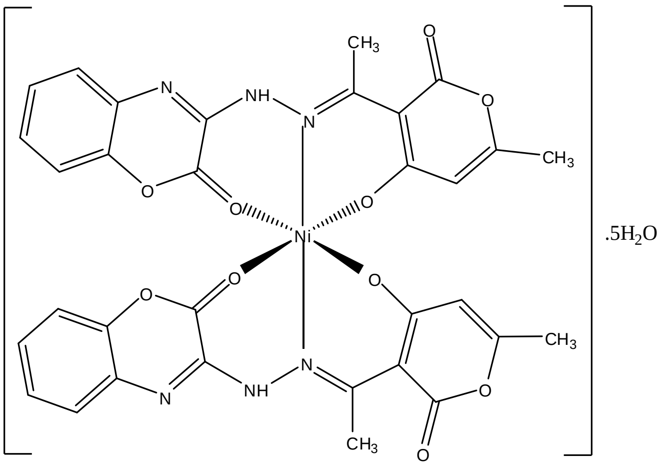

Ni (II) complex

Figure 10. Proposed Structure of Ni (II) complex

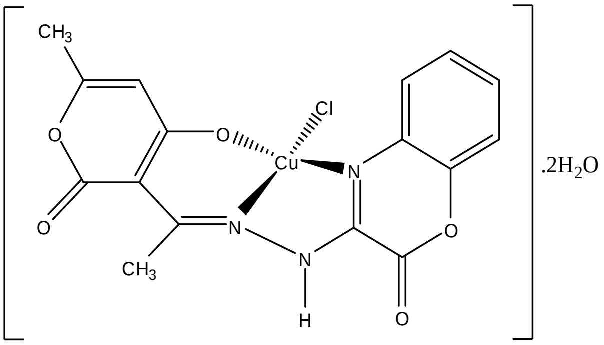

Cu (II) complex

Figure 11. Proposed Structure of Cu (II) complex

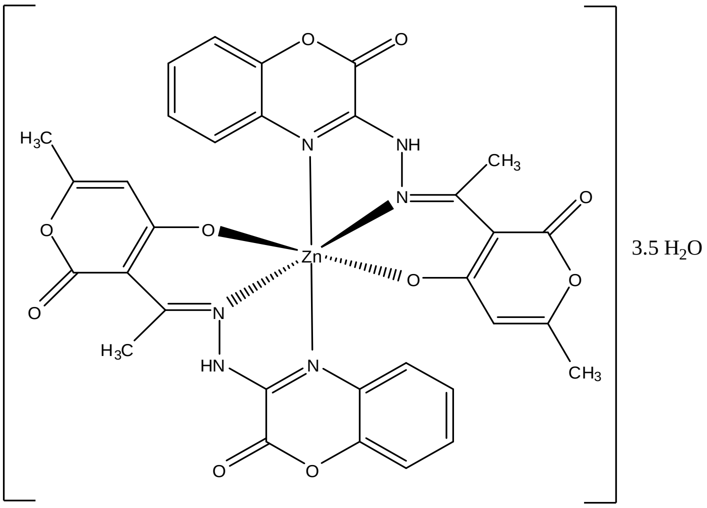

Zn (II) complex

Figure 12. Proposed Structure of Zn (II) complex

Acknowledgements

We are thankful to the DST-FIST Program of India (SR/FST/CSI-213/2010) for providing the infrastructural facilities, Department of Chemistry, University College for Women, Osmania University and also DST-FIST Program of India (SR/FST/CSI-210/2010) for providing the instrumental facilities, Department of Chemistry, University College of Science, Osmania University, Hyderabad.

REFERENCES

[1] R. Fringuelli, D. Pietrella, F. Schiaffella, A. Guarraci, S. Perito, F. Bistonib, A. Vecchiarellib, *Bioorgan. Med. Chem*., **2002**, 10 (6), 1681.
[2] S. Alper-Hayta, E. Aki-Sener, B. Tekiner-Gulbas, I. Yildiz, O. Temiz-Arpaci, I. Yalcin, N. Altanlar, *Eur. J. Med. Chem.*, **2006**, 41 (3), 398.
[3] N. Siddiquia, R. Alia, M. Shamsher Alama, W. Ahsana, *J. Chem. Pharm. Res.*, **2010**, 2 (4), 309.
[4] P. Depreux, Z. Moussavi, D. Lesieur, Sauzieres, *J. Farmaco.*, **1993**, 48 (8), 1079.
[5] P. Mizar, B. Myrboh, *Tetrahedron Lett*., **2006**, 47 (44), 7823.
[6] B. Schleiffenbaum, O. Spertini, F. Tedder Thomas, *J. Cell. Biol*., **1992**, 119 (1), 229.
[7] V. G. Stanley, S. Woldesenbet, G. Cassandra, *Poultry Sci.*, **1996**, 75 (1), 42.
[8] S. M. Achut, N. J. Amarnath, M.J. Sarika, K.C. Trimbak, *J. Serb. Chem. Soc*., **2010**, 75 (3), 349.
[9] A. Levai, J. Jeko, *Monatsh Chem.*, **2006**, 137, 339.
[10] R. K. Agarwal, L. Singh, D. K. Sharma, R. Singh, *Turk. J. Chem.*, **2005**, 29 (3), 309.
[11] B.N. Figgis, J. Lewis, *Modern Coordination Chemistry,* Interscience Inc, New York, **1960**, 403.
[12] B. Loev, H. Jones, R.E. Brown, F.C. Huang, A. Khandwala, M.J. Leibowitz, P.S. Goldman, *J. Med. Chem*., **1985**, 28 (1), 24.
[13] V. Haribabu, P.V. Anantha Lakshmi, V. Jayatyaga Raju, *Der Pharma Chemica,* **2011**, 3 (4), 413.
[14] R.M. Silverstine, G.C. Bassler, T.C. Morill, *Spectrometric identificaion of organic compounds*, John Wiley and Sons, New York, **1991**.
[15] A.S. Munde, A.N. Jagdale, S. M. Jadhav, Chondhekar, T. K. *J. Serb. Chem. Soc*., **2010**, 75 (3), 349.
[16] P.V. Anantha Lakshmi, B.S. Shyamala, V. Jayatyaga Raju, *Polish J. Chem*. **2009**, 83 (9), 1555.
[17] N.S. Gwaram, H. M. Ali, H. Khaledi, M. A. Abdulla, A.H.A. Hadi, T.L Lin, C. L. Ching, C. L. Ooi, *Molecules*, **2012**, 17 (5), 5952.
[18] A. Sharma, T. Mehta, M. K. Shah, *Der Chemica Sinica,* **2013**, 4 (1), 141.
[19] CH. Thirupataiah, D. P. Chary, M. Ravinder, S. Srihari, *Oriental J. Chem.,* **2008**, 24, 859.
[20] P.V. Anantha Lakshmi, P. Saritha Reddy, V. Jayatyaga Raju, *Bull. Chem. Soc. Ethiop*., **2008**, 22 (3), 385.
[21] A.S. Shayma, F. Yang, A. S. Abbas, *Eur. J. Sci. Res*., **2009**, 33 (4), 702.
[22] P. Tharmaraj, D. Kodimunthiri, C.D. Sheela, C.S. Shanmuga Priya, *J. Serb.Chem. Soc*., **2009**, 74 (8-9), 927.
[23] B. Manjula, S. Arul Antony, *Asian J. Biochem. Pharm. Res*., **2013**, 3 (1), 168.
[24] W.J. Geary, *Coordin. Chem. Rev.,* **1971**, 7, 81.
[25] D. Sandhya Rani, P.V. Anantha Lakshmi, V. Jayatyaga Raju, *Res. J. Pharm. Bio. Chem. Sci.,* **2014**, 5 (2), 1304.
[26] P. Saritha reddy, P.V. Ananthalakshmi, V. Jayatyagaraju, *E-Journal of Chem.*, **2011,** 8 (1), 415.
[27] V. Haribabu, P.V. Anantha Lakshmi, V. Jayatyaga Raju, *Int. J. Chem Tech Res*., **2013**, 5 (4), 1512.
[28] H.A. Bayoumi, M.A. Abdel-Nasser Alaghaz, sh. Mutlak Aljahdali, *Int. J. Electrochem. Sci*., **2013**, 8, 9399.
[29] L.S. Prabhumirashi, J. K. Khoje, *Thermochim. Acta*., **2002**, 383 (1), 109.
[30] L.V. Ababei, A. Kriza, C. Andronescu, A.M. Musuc, *J. Serb. Chem. Soc*., **2011**, 76 (8), 1103.
[31] P.V. Anantha Lakshmi, P. Saritha Reddy, V. Jayatyaga Raju, *Spectrochim. Acta A*., **2009**, 74 (1), 52.
[32] A.A. Pawanoji, B.H. Mehta, *Asian J. Chem*., **2009,** 21 (9), 6869.
[33] J.M. Seco, M. Quiros, M.J.G. Garmendia, *Polyhedron*, **2000**, 19 (8), 1005.
[34] M. Thankamony, K. Mohanan, *Indian J. Chem*., **2007**, 46A, 247.
[35] K.R. Kumar, A.R. Guru Prasad, V. Srilalitha, G. N. Swami, L.K. Ravindranath, *Chem. Bull. Politehnica Univ., (Timisoara),* **2012**, 57 (71) (1), 7.
[36] D. Sandhya Rani, P.V. Anantha Lakshmi, V. Kamala Prasad, V. Jayatyaga Raju, *Chinese j. inorg. chem*., **2012**, 28 (6), 1245.
[37] P.P. Hankare, S.R. Naravane, V.M. Bhuse, S.D. Delekar, A.H. Jagtap, *Indian J. Chem.,* **2004**, 43A, 1464.
[38] F.A. Cotton, G. Wilkinson, *Advanced inorganic chemistry*; New York, Wiley Interscience, **1962**.
[39] N. Raman, J. Dhaveethu Raja, A. Sakthivel *, J. Chem. Sci*., **2007**, 119 (4), 303.
[40] N. Raman, S.J. Raja, J. Joseph, J. D. Raja, *J. Chil. Chem. Soc*., **2007**, 52 (2), 1138.
[41] S.G. Shirodkar, P.S. Mane, T.K. Chondhekar, *Indian J. Chem*., **2001**, 40A, 1114.
[42] P.W. Selwood, *Magnetochemistry,* Interscience, New York, London, **1956**, 226.
[43] A.B.P. Lever, *Inorganic electronic spectroscopy,* Elsevier, Amsterdam, the Netherlands, **1984**.
[44] L.F. Lindoy, W.E. Moody, D. Taylor, *Inorg. Chem*. **1997**, 16, 1962.
[45] Nursen Sari, Perihan Gurkan, *Z. Naturforsch.,* **2004**, 59b, 692.
[46] B.K. Kumar, V. Ravinder, G.B. Swamy, S.J. Swamy, *Indian J. Chem*., **1994**, 33A, 136.
[47] M.N. Patel, V.J. Patel, *Syn. React. Inorg. Met.,* **1989**, 19 (2), 137.
[48] R.K. Ray, G.B. Kauffman, *Inorg. Chem. Acta*., **1990**, 173, 207.
[49] N. Raman, A. Kulandaisamy, K. Jeyasubramanian, *Indian J. Chem*. **2002**, 41A, 942.
[50] N. Raman, V. Muthuraj, S. Ravichandran, A. Kulandaisamy, *Proc. Indian Acad. Sci., (Chem. Sci.),* **2003**, 115 (3), 161.

[51] N. Raman, T. Baskaran, A. Selvan, R. Jeyamurugan, *J. Iran. Chem. Res.*, **2008**, 1, 129.
[52] M. Joseph, M. Kuriakose, M.R.P. Kurup, E. Suresh, A. Kishore, S.G. Bhat, *Polyhedron,* **2006**, 25 (1), 61.
[53] I.M. Procter, B.J. Hathaway, P. Nicholls, *J. Chem. Soc. A*, **1968**, 1678.
[54] E.B. Seena, R. Maliyeckal Prathapachandra Kurup, *Polyhedron*, **2007**, 26 (4), 829.
[55] N. Raman, Y. Pitchaikani Raja, A. Kulandaisawy, *Proc. Indian Acad. Sci. (Chem. Sci.),* **2001**, 113 (3), 183.
[56] O. Turkoglu, M. Soylak, I. Belenli, *Collect. Czech. Chem. Comm.*, **2003**, 68 (7), 1233.